FULL PAPER

BJC

British Journal of Cancer (2017) 117, 1621–1630 | doi: 10.1038/bjc.2017.319

Keywords: ailanthone; non-small cell lung cancer; DNA replication; RPA1; Chinese medicine

Ailanthone inhibits non-small cell lung cancer cell growth through repressing DNA replication via downregulating RPA1

Zhongya Ni[1], Chao Yao[1], Xiaowen Zhu[1], Chenyuan Gong[1], Zihang Xu[2], Lixin Wang[3], Suyun Li[4], Chunpu Zou[2] and Shiguo Zhu[*,1,3]

[1]*Laboratory of Integrative Medicine, School of Basic Medical Sciences, Shanghai University of Traditional Chinese Medicine, 1200 Cai Lun Rd, Shanghai 201203, PR China;* [2]*Department of Internal Classic of Medicine, School of Basic Medical Sciences, Shanghai University of Traditional Chinese Medicine, 1200 Cai Lun Rd, Shanghai 201203, PR China;* [3]*Department of Immunology and Pathogenic Biology, School of Basic Medical Sciences, Shanghai University of Traditional Chinese Medicine, 1200 Cai Lun Rd, Shanghai 201203, PR China and* [4]*Department of Pathology, School of Basic Medical Sciences, Shanghai University of Traditional Chinese Medicine, 1200 Cai Lun Rd, Shanghai 201203, PR China*

Background: The identification of bioactive compounds from Chinese medicine plays a crucial role in the development of novel reagents against non-small cell lung cancer (NSCLC).

Methods: High throughput screening assay and analyses of cell growth, cell cycle, apoptosis, cDNA microarray, BrdU incorporation and gene expression were performed.

Results: Ailanthone (Aila) suppressed NSCLC cell growth and colony formation *in vitro* and inhibited NSCLC tumour growth in subcutaneously xenografted and orthotopic lung tumour models, leading to prolonged survival of tumour-bearing mice. Moreover, Aila induced cell cycle arrest in a dose-independent manner but did not induce apoptosis in all NSCLC cells. Furthermore, 1222 genes were differentially expressed upon Aila administration, which were involved in 21 signal pathways, such as DNA replication. In addition, Aila dose-dependently decreased BrdU incorporation and downregulated the expression of replication protein A1 (RPA1).

Conclusions: Aila inhibited the growth of NSCLC cells through the repression of DNA replication via downregulating RPA1, rather than through cell cycle arrest and apoptosis. Our findings suggested that Aila could be used as a promising therapeutic candidate for NSCLC patients.

Lung cancer is the leading cause of cancer death worldwide and non-small cell lung cancer (NSCLC) is the most common type and represents 80% of all lung cancers. In China, approximately 4 292 000 new cancer cases and 2 814 000 cancer deaths occurred in 2015, and lung cancer is also the most common cancer and the leading cause of cancer death (Chen *et al*, 2015). Although the 5-year survival rate has been improved owing to the advances in the management of NSCLC over the past 30 years, the overall 5-year survival rate is still less than 5%. Therefore, it is emergently necessary to develop novel treatment strategies to improve efficiency and reduce mortality of lung cancer.

Natural products are a major resource for the development of novel drug leads (Cragg and Newman, 2013). Chinese medicine has been extensively documented over the centuries, which has a long history of use in cancer treatment, showing significantly improved therapeutic efficacy, reduced side effects of

*Correspondence: Dr S Zhu; E-mail: zhushiguo@shutcm.edu.cn

Received 8 June 2017; revised 10 August 2017; accepted 18 August 2017; published online 12 October 2017

chemotherapy and prolonged survival (He *et al*, 2016a; Zheng *et al*, 2017). Therefore, the identification of bioactive compounds from Chinese medicine plays a crucial role in the development of new anticancer reagents.

In the present study, high throughput screening assay showed that ailanthone (Aila) possessed the potential to inhibit NSCLC cell growth. Aila is a main active compound of the stem barks of *Ailanthus altissima*, which is traditionally used to treat ascariasis, diarrhoea, spermatorrhoea, bleeding and gastrointestinal diseases, and it has been recently found to have anti-inflammatory and anti-tumour activities (Kim *et al*, 2015; Wang *et al*, 2016). Analyses of cell growth, cell cycle, apoptosis, cDNA microarray, BrdU incorporation and gene expression revealed that Aila could significantly inhibit NSCLC cell growth both *in vitro* and *in vivo*. Moreover, Aila repressed DNA replication in a dose-dependent manner and significantly downregulated replication protein A1 (RPA1). This finding indicated that Aila inhibited NSCLC cell growth through targeting replication stress, suggesting that Aila could be used as a promising therapeutic candidate in NSCLC treatment.

MATERIALS AND METHODS

Reagents. Aila was purchased from BioBioPha Co., Ltd (Yunnan, China). Cell cycle kit was obtained from Biotime (Beijing, China). Annexin V-FITC apoptosis kit and bromodeoxyuridine (BrdU) flow cytometry kit were supplied from BD Biosciences (San Jose, CA, USA). RNA extraction kit, PrimeScript RT MasterMix kit and SYBR Premix Ex Taq kit were provided by Takara (Dalian, China). Antibodies against caspase-3, PARP (poly ADP-ribose polymerase) and actin as well as secondary antibodies were purchased from Cell Signaling Technology (Danvers, MA, USA). Antibodies against RPA1 and proliferating cell nuclear antigen (PCNA) were obtained from Santa Cruz (CA, USA). Mouse anti-human γ-H2AX monoclonal antibody and goat anti-mouse IgG Alexa Fluro 488 were purchased from Abcam (Cambridge, MA, USA). ECL western blotting substrate kit was supplied from Merck Millipore (Billerica, MA, USA). Amaxa cell line nucleofector kit T was purchased from Lonza (Cologne, Germany). MTT assay kit, cisplatin (DDP) and camptothecin (CPT) were provided by Sigma-Aldrich (St Louis, MO, USA).

Cell culture. Human NSCLC A549, H1299 and H1975 cell lines were obtained from Shanghai Cell Bank of Chinese Academy of Sciences. A549 cells were cultured in high glucose DMEM (Gibco, Life Technologies, Grand Island, NY, USA) supplemented with 10% foetal bovine serum (FBS; Gibco) and 1% penicillin and streptomycin in 5% CO_2. H1299 and H1975 cells were cultured in RPMI 1640 (Gibco) supplemented with 10% FBS and 1% penicillin and streptomycin in 5% CO_2.

Cell viability assay. MTT assay was performed to determine the effect of Aila on the viability of NSCLC cells. Briefly, A549, H1299 and H1975 cells were respectively seeded in 96-well plates at a density of 4×10^3 cells per well. Aila or DDP was added to the cells at different final concentrations (0, 0.078, 0.156, 0.3125, 0.625, 1.25, 2.5, 5.0, 10 and 20 μM). At 24, 48 and 72 h, MTT was added to the cells at a final concentration of 0.5 mg ml^{-1}. After 4 h of incubation, the medium was aspirated, and an equal volume of DMSO was added to dissolve the formazan precipitate. Plates were read at a wavelength of 490 nm using Synergy 2 Multi-Mode Microplate Reader (BioTek Instrument, Int., Winooski, VT, USA). Independent experiments were performed at least three times.

Colony formation assay. Colony formation assay was performed to further determine the effect of Aila on NSCLC cell tumourigenicity. A549, H1299 and H1975 cells were respectively seeded in six-well plates at a density of 200 cells per well. Aila was added to the cells at different final concentrations (0, 0.078 and 0.156 μM), and then the cells were incubated for 12 days. The colonies were fixed by 4% paraformaldehyde for 15 min, stained with crystal violet for 15 min and then imaged and counted under a phase-contrast microscope.

Subcutaneous xenograft tumour models. All animal procedures, including tumour transplantation, tumour volume monitoring and killing, were approved by the Institutional Animal Care and Use Committee at Shanghai University of Traditional Chinese Medicine. For subcutaneous xenograft model, male Balb/c nude mice (6–8-week-old, weighing 18–20 g) were purchased from Shanghai SLAC Laboratory Animal Co., Ltd (Shanghai, China) and maintained under an SPF environmental condition. Briefly, 3×10^6 of H1975 cells or A549 cells were subcutaneously inoculated in the back of nude mice. When tumour volume reached approximately 100 mm^3, mice were randomly assigned and administered with different doses of Aila via intraperitoneal (IP) injection. The tumour volume and body weight were determined every 3 days. Tumour volume was calculated using the following formula: $V = (\pi/8)a \times b^2$, where V = tumour volume, a = maximum tumour diameter and b = minimum tumour diameter. Mice were humanely killed by CO_2 suffocation when the tumour volume reached 2000 mm^3.

Biochemistry and histology. To evaluate the safety of Aila, mice in the subcutaneous xenograft model were killed on day 58, and serum, liver and kidney were collected. Serum levels of alanine aminotransferase (ALT), aspartate aminotransferase (AST), albumin (ALB) and creatinine (CREA) were determined. Liver and kidney were fixed with 10% fresh formalin, embedded in paraffin, cut into 4-μm sections, stained with haematoxylin–eosin and then observed under a light microscope ($\times 100$ and $\times 400$ magnification).

Orthotopic lung tumour models and bioluminescent imaging. Male SCID-Bg mice (6–8-week-old) were purchased from Vital River Laboratory Animal Technology Co. (Beijing, China) and maintained under an SPF environmental condition. Mice were anaesthetised with 0.5% mebubarbital, and the left chest was shaved and exposed. Briefly, 1×10^6 eGFP-FFLuc + A549 cells in 50 μl serum-free DMEM medium were mixed with 50 μl matrigel, and then the mixture was injected into the left lung. On day 4 after injection, mice were treated with 2 mg kg^{-g} of Aila via IP administration every 3 days, and the tumour volume was weekly monitored by imaging isoflurane-anaesthetised mice using the IVIS system (Xenogen, Alameda, CA, USA).

Cell cycle analysis. A total of 3×10^5 of A549, H1299 and H1975 cells were respectively seeded in 6-cm plates and incubated overnight. Cells were then incubated with different concentrations (0, 0.625, 1.25, 2.5 and 5.0 μM) of Aila for 24 h. Subsequently, cells were harvested, washed with ice-cold PBS, then fixed with 70% ethanol overnight at −20 °C and stained with propidium iodide (PI) at 37 °C for 30 min in the dark. The DNA content was determined using a FACS Calibur cytometer (BD Biosciences) and analysed by the FCS Express v2.0 software (De Novo Software, Glendale, CA, USA). The cell cycle distribution was determined by ModFit software (Verity, Software House, Topsham, ME, USA).

Apoptosis analysis. A total of 3×10^5 of A549, H1299 and H1975 cells were respectively seeded in 6-cm plates and incubated with different concentrations (0, 0.625, 1.25, 2.5 and 5.0 μM) of Aila for 12 h. The cells were then harvested, washed and stained with FITC-Annexin V and PI according to the manufacturer's protocols. Apoptosis was assessed using a C6 flow cytometer (BD Biosciences) and analysed by FlowJo (Ashland, OR, USA).

DNA damage assay. A total of 3×10^5 of A549, H1299 and H1975 cells were, respectively, seeded in 6-cm glass bottom dishes and incubated with different concentrations (0, 0.625, 1.25, 2.5 and 5.0 μM) of Aila or 5 μM of CPT for 24 h. Cells were fixed with 4% paraformaldehyde for 20 min, treated with 1% Triton for 20 min and incubated with anti-H2AX antibody at 4 °C overnight. The cells were then incubated with Alexa Fluro 488 anti-mouse antibody for 30 min and stained with DAPI for 20 min. Images were captured by laser confocal microscopy.

Microarray gene expression analysis. Differential gene expression was examined by cDNA microarray to investigate the molecular mechanism of action (MOA). A549, H1299 and H1975 cells were, respectively, treated with 1.25 μM Aila for 24 h. Total RNA was extracted using the Trizol reagent (Invitrogen, Life Technologies) and reversely transcribed into complementary DNA (cDNA) using the Quantscript RT kit (Tiangen Biotech, Beijing, China). Hybridisation was performed by Shanghai Biotechnology Corporation (Shanghai, China) using the Agilent SurePrint G3 Human Gene Expression Microarray 8×60K, which contains 56 689 probes per array product. Normalised algorithms were used to transform sample signals to minimise the effects of variation from non-biological factors. Analysis of gene expression profiles was completed by the Illumina BeadStudio module application (Illumina Inc., San Diego, CA, USA). Genes with fold change $\geqslant 2$ and $P \leqslant 0.05$ were identified as differentially expressed genes (DEGs) between Aila-treated group and controls. Gene ontology (GO) analysis of DEGs was performed with GO categories (http://www.geneontology.org).

BrdU flow cytometry. To determine DNA replication by Aila, BrdU incorporation and fluorochrome-labelled antibody detection were applied to detect the newly synthesised DNA of replicating cells during the S phase of the cell cycle. Briefly, 3×10^5 of A549, H1299 and H1975 cells were respectively seeded in six-cm plates and incubated overnight. Subsequently, cells were treated with different concentrations (0, 0.625, 1.25, 2.5 and 5.0 μM) of Aila for 24 h. The cells were then harvested, pulsed with BrdU for 1 h, rinsed and treated with DNAase at 37 °C for 1 h, followed by staining with FITC anti-BrdU for 20 min and 7-AAD for 20 min at room temperature in the dark. The BrdU incorporation in replicating cells during S phase was measured using C6 flow cytometer (BD Biosciences) and analysed by FlowJo (USA).

Real-time PCR. A total of 3×10^5 of A549, H1299 and H1975 cells were, respectively, seeded in 6-cm plates and incubated with different concentrations (0, 0.625 and 1.25 μM) of Aila for 24 h. Total RNA was extracted using MiniBEST Universal RNA extraction kit (Takara), and 1 μg of total RNA was reversely transcribed into cDNA using the PrimeScript RT MasterMix kit (Takara) according to the manufacturer's instructions. Real-time PCR was performed using SYBR Premix Ex Taq kit (Takara) according to the manufacturer's instructions on an ABI system (Applied Biosystems, Life Technologies). After a denaturation step at 95 °C for 30 s, amplifications were carried out with 40 cycles at a melting temperature of 95 °C for 5 s and an annealing temperature of 60 °C for 30 s, followed by melt curve analysis. The relative expression was calculated using the $2^{-\Delta\Delta Ct}$ method. Primers for all genes were listed as follows: 18S forward: 5′-GTAACCCGTTGAACCCCATT-3′; 18S reverse: 5′-CCATCCAATCGGTAGTAGCG-3′; PCNA forward: 5′-TCAGGTACCTCAGTGCAAAAG-3′; PCNA reverse: 5′-TGCAAGTGGAGAACTTGGAA-3′; RPA1 forward: 5′-CCAGTGCCCTATAATGAAGGA-3′; RPA1 reverse: 5′-CCATTCCCGAGCTTCCAT-3′; POLE2 forward: 5′-TTTTGCAGAAGTCTTCACAGATG-3′; POLE2 reverse: 5′-GCAGAAGGTTGGTTTGAAGA-3′; LIG1 forward: 5′-CTCTCCCATCTACCCTGCTG-3′; LIG1 reverse: 5′-TAAACCGAGGGAAGCGAAG-3′.

Western blot. A549, H1299 and H1975 cells were respectively seeded in 10-cm plates and incubated with different concentrations (0, 0.625, 1.25, 2.5 and 5.0 μM) of Aila for 24 h. The cells were then lysed with RIPA lysis buffer, and protein contents were quantitated using BCA protein reagent assay kit (Yeasen, Shanghai, China) and analysed by 8–10% of SDS–PAGE, followed by immunoblotting using enhanced chemiluminescence substrate (Merck Millipore) according to the manufacturer's instructions. Bands were visualised using a chemiluminescent detection system (ProteinSimple, San Jose, CA, USA).

RPA1 overexpression assay. The coding sequence of RPA1 (NM_002945.3) was amplified by PCR using the primers as follows: forward: 5′-CGCTTAAGCCACCATGGTCGG-3′; reverse: 5′-CGGGATCCGTCACATCAATGCAC-3′. The amplicons were then inserted into the cloning sites of *Afl*II and *Bam*HI between CMV promoter and IRES-EGFP sequences in EGFP-FFLuc-HyTk-pMG^pac (a gift from Dr Dean Anthony Lee) to construct RPA1 overexpression vector. RPA1 plasmid DNA and control vector were respectively transfected into A549 and H1299 cells by using Nucleofector II device. After 72 h, RPA1 expression in A549 and H1299 cells was respectively detected by western blot analysis, and cell viability by Aila was accessed as described in cell viability assay.

Statistical analysis. Data were expressed as means ± standard deviation (s.d.), and $P < 0.05$ was considered statistically significant. The tumour volume and survival were determined using repeated measure of general linear model and log-rank test by SPSS 18.0, respectively. Other statistical analyses were performed using the Student's *t*-test and one-way analysis of variance (ANOVA).

RESULTS

Aila inhibits NSCLC cell growth and colony formation. To identify active compounds from Chinese medicine that may inhibit NSCLC cell growth, we screened 3000 herbal monomers by an ATP luminescent high throughput assay. We found that the herbal monomer Aila, a natural product from the stem barks of *A. altissima*, possessed the potential to inhibit NSCLC cell growth. To confirm this finding, we assessed the effect of Aila on the growth and colony formation of NSCLC cells. Results showed that Aila significantly inhibited the growth of A549, H1299 and H1975 cells (Figure 1A). Moreover, it clearly reduced the colonies (Figure 1B and C). Furthermore, Aila elicited a better inhibitory effect than DDP, which is the first-line chemotherapy for NSCLC (Supplementary Figure S1). These results clearly demonstrated that Aila inhibited NSCLC cell growth and colony formation in a dose- and time-dependent manner, suggesting that Aila was a potential candidate for NSCLC treatment.

Aila suppresses subcutaneously xenografted and orthotopic lung tumour growth. Since Aila significantly inhibited the NSCLC cell growth *in vitro*, we next investigated its inhibitory effect *in vivo*. Mice with H1975 cell subcutaneous xenograft tumour were treated with 1 or 2 mg kg^{-1} of Alia every 3 days via IP injection from day 3. Results showed that Aila significantly inhibited H1975 cell tumour growth (Figure 2A), the body weight of mice was not changed (Supplementary Figure S1A) and the median survival time for 0, 1 and 2 mg kg^{-1} of Aila treatment groups was 30, 40.5 and 48 days, respectively (Figure 2B). Mice with A549 cell subcutaneous xenograft tumour were then treated with 2 mg kg^{-1} of Aila to determine the effect of Aila on other NSCLC cells, and similar results were obtained (Supplementary Figure S1B). Mice treated with 2 mg kg^{-1} of Aila were killed, and the tumours of Aila-treated mice were much smaller (Supplementary Figure S2C and D) and lighter (Supplementary Figure S2E and F) compared with vehicle-

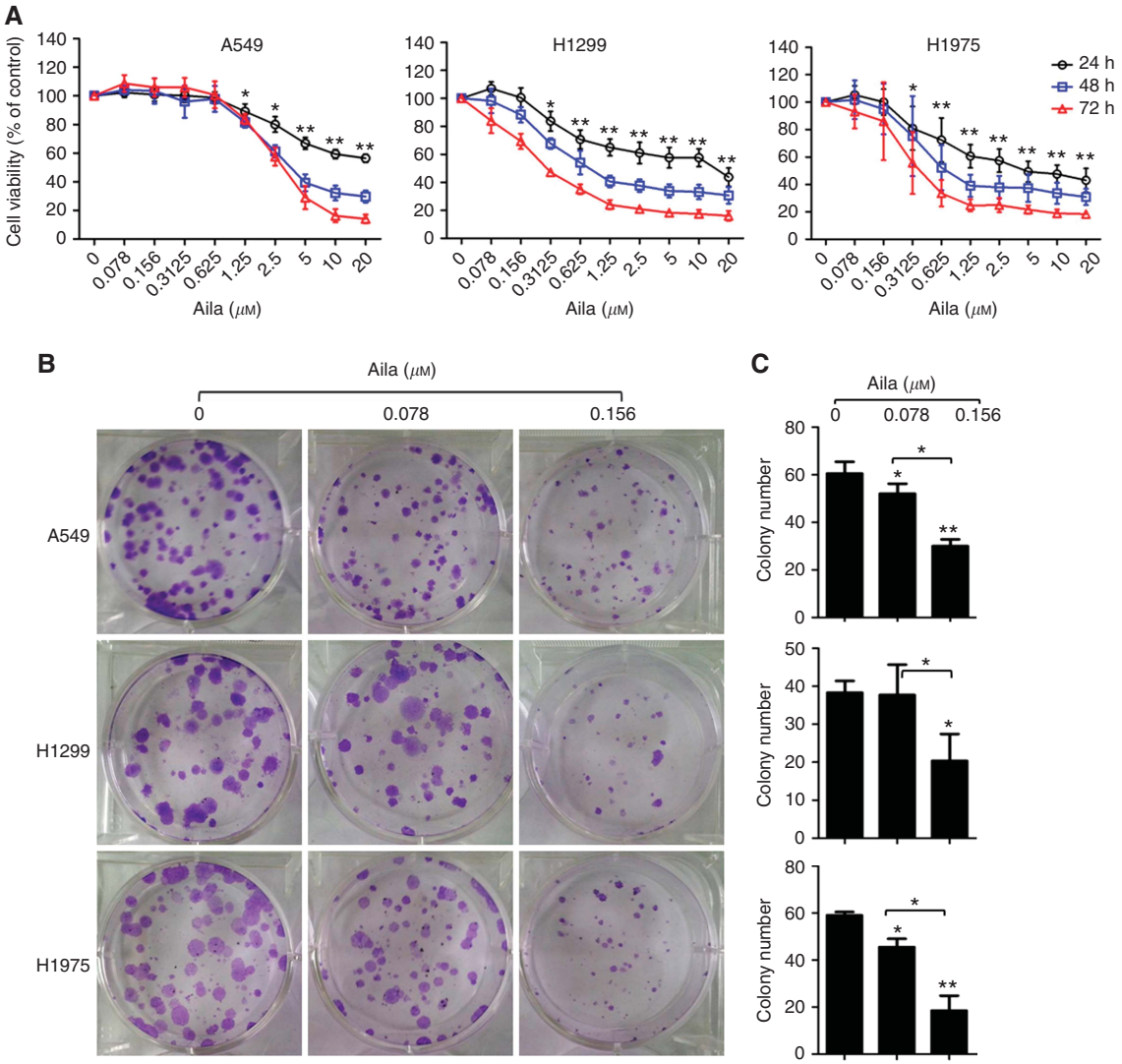

Figure 1. Aila inhibits NSCLC cell growth and colony formation. (**A**) A549, H1299 and H1975 cells were treated with Aila at different concentrations (0, 0.078, 0.156, 0.3125, 0.625, 1.25, 2.5, 5.0, 10 and 20 μM). At 24, 48 and 72 h, MTT assay was performed and cell viability was analysed. Data were pooled from three independent experiments. (**B**) A549, H1299 and H1975 cells were treated with Aila at different concentrations (0, 0.078 and 0.156 μM) for 12 days. Colonies were stained with crystal violet. (**C**) Data were pooled from three independent experiments. *$P<0.05$; **$P<0.01$.

treated mice. The serum levels of ALT, AST, ALB and CREA had no significant difference (Supplementary Figure S3A), and no clear damage was found in liver and kidney after Aila treatment (Supplementary Figure S3B). We further investigated the efficacy of Aila in an orthotopic eGFP-FFLuc+ A549 cell tumour model by bioluminescent imaging. Results showed that Aila clearly inhibited orthotopic lung tumour growth (Figure 2C and D), and the median survival time for vehicle- and Aila-treated mice was 35 and 55 days (Figure 2E), respectively. Taken together, these results demonstrated that Aila could significantly inhibit NSCLC cell growth *in vitro* and tumour growth *in vivo* with low toxicity, leading to prolonged survival of tumour-bearing mice.

Aila dose-independently induces cell cycle arrest. Since Aila showed a clear inhibitory effect on NSCLC cell tumour growth both *in vitro* and *in vivo*, we next determined the biological MOA. Cell cycle arrest is usually induced by lots of anticancer reagents and was investigated in our study. Results showed that the G2 phase was significantly increased in A549 cells, while G1 phase was significantly increased in H1299 and H1975 cells after Aila treatment (Figure 3A and B). Unexpectedly, these reductions were dose-independent. These results showed that Aila dose-independently induced classic G1 or G2/M arrest in NSCLC cells, suggesting that classic cell cycle arrest was not crucial for Aila to suppress NSCLC cells.

Aila induces apoptosis in H1975 cells, but not in A549 and H1299 cells. Our study showed that cell cycle arrest might be not crucial for Aila to suppress NSCLC cells, and Aila has been recently shown to induce apoptosis in liver cancer (Zhuo *et al*, 2015). Therefore, we determined apoptosis in NSCLC cells. Results showed that early apoptotic (Annexin V+PI−) cells were significantly increased in H1975 cells in a dose-dependent manner, but not in A549 and H1299 cells (Figure 4A and B). Further analysis by western blotting showed that caspase-3 and PARP were cleaved by Aila in H1975 cells, but not in A549 and H1299 cells (Figure 4C). We also investigated the DNA damage and found that Aila induced DNA damage in H1299 and H1975 cells, but not in A549 cells (Supplementary Figure S4). Taken together, these results showed that Aila did not induce apoptosis and DNA damage in all NSCLC cells, suggesting that apoptosis and DNA damage were not necessary for Aila to inhibit NSCLC cell growth.

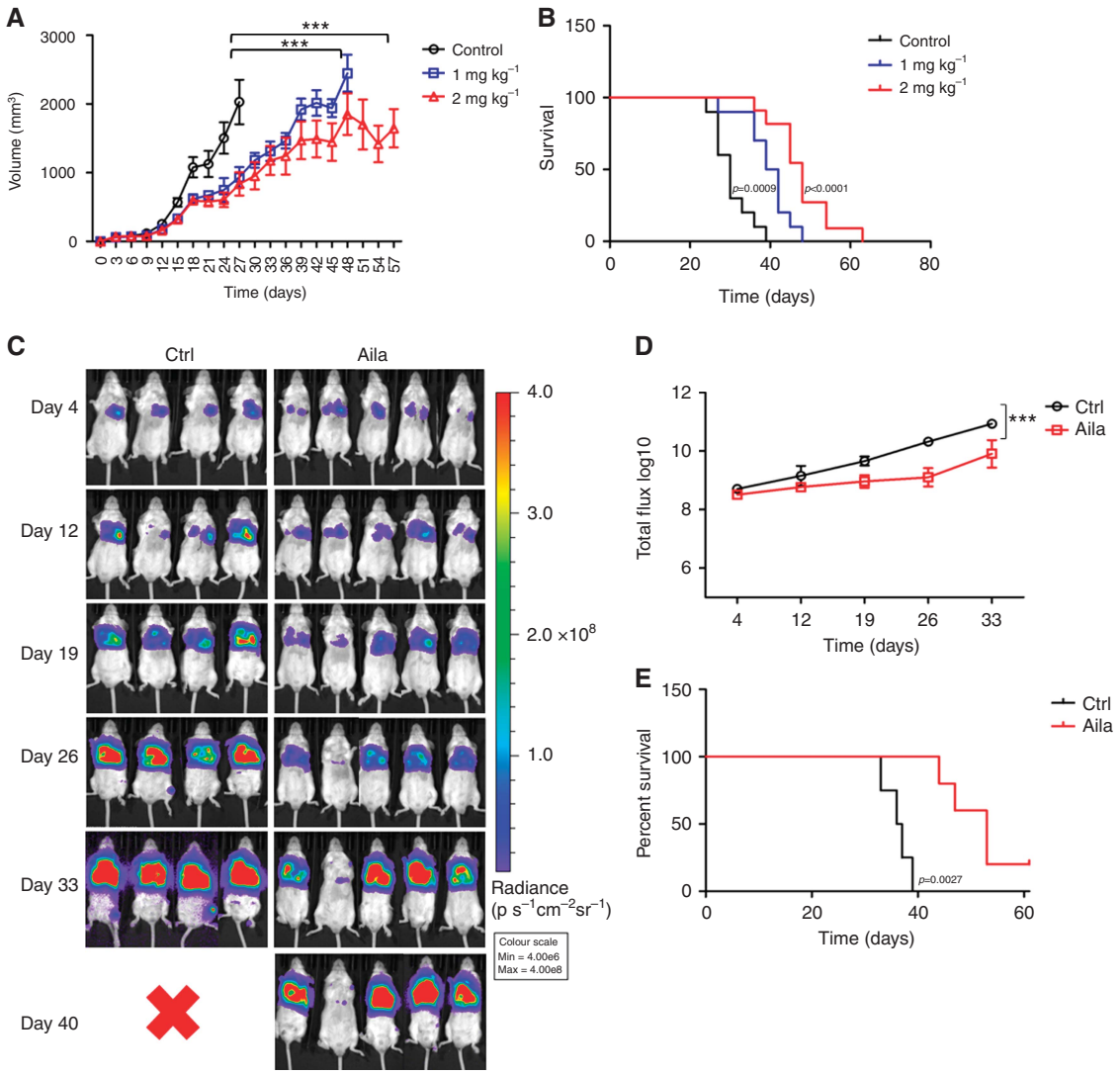

Figure 2. Aila inhibits subcutaneously xenografted and orthotopic lung tumour growth and prolongs survival of tumour-bearing mice. H1975 cells were subcutaneously inoculated in the back of nude mice to generate xenograft tumour model, or eGFP-FFluc+ A549 cells were injected into the left lung to establish orthotopic lung tumour model. (**A**) H1975 cell tumour growth. (**B**) Survival rate of H1975 cell-bearing mice. (**C**, **D**) Orthotopic tumour size. (**E**) Survival rate of orthotopic tumour-bearing mice. Tumour growth graph represents two independent experiments, and the survival curve was pooled from two independent experiments. ***$P<0.001$.

Aila induces 1222 DEGs involving in 21 signal pathways. Above-mentioned results showed that cell cycle arrest and apoptosis were not crucial for Aila to inhibit NSCLC cells. A cDNA microarray was applied to further elucidate the major MOA. Results showed that a total of 6124 genes in A549 cells, 4386 genes in H1299 cells and 10 680 genes in H1975 cells were differentially expressed upon Alia administration. Among these genes, 3212 genes were upregulated and 2912 genes were downregulated in A549 cells; 2351 genes were upregulated and 2035 genes were downregulated in H1299 cells; and 5898 genes were upregulated and 4782 genes were downregulated in H1975 cells. Moreover, 1222 genes were significantly differentially expressed in A549, H1299 and H1975 cells simultaneously (Figure 5A). Among these genes, 732 genes were upregulated and 490 genes were downregulated. GO analysis demonstrated that 21 signal pathways were significantly regulated in three types of cells (Figure 5B). Interestingly, nucleotide excision repair and DNA replication pathways, both are crucial for accurate DNA replication during cell cycle S phase, were included in these pathways. Totally four genes, PCNA, RPA1, human DNA polymerase epsilon B-subunit (POLE2) and DNA ligase I (LIG1), were involved in both nucleotide excision repair and DNA replication signalling pathways. These results suggested that Aila might repress DNA replication through downregulating PCNA, RPA1, POLE2 and LIG1.

Aila represses DNA replication. BrdU, a halogenated nucleoside, serves as a thymidine analogue and has been frequently used as a tracer of *de novo* DNA synthesis (Tada and Grossart, 2013). Therefore, BrdU flow cytometry was carried out to confirm the microarray result. Results showed that the S phase was dramatically decreased from 46.6% to 26.0%, 10.4%, 1.79% and 0.387% in A549 cells, from 42.1% to 21.1%, 7.37%, 0.911% and 0.199% in H1299 cells, and from 11.7% to 0.522%, 0.124%, 0.244% and 0.150% in H1975 cells in a dose-dependent manner after Aila treatment of 0.625, 1.25, 2.5 and 5.0 μM, respectively (Figure 5C). Moreover, such reductions were significant (Figure 5D). These results clearly demonstrated that Aila decreased the BrdU incorporation of the newly synthesised DNA of replicating cells during the S phase of the cell cycle in a dose-dependent manner in NSCLC cells, implying that Aila inhibited DNA replication.

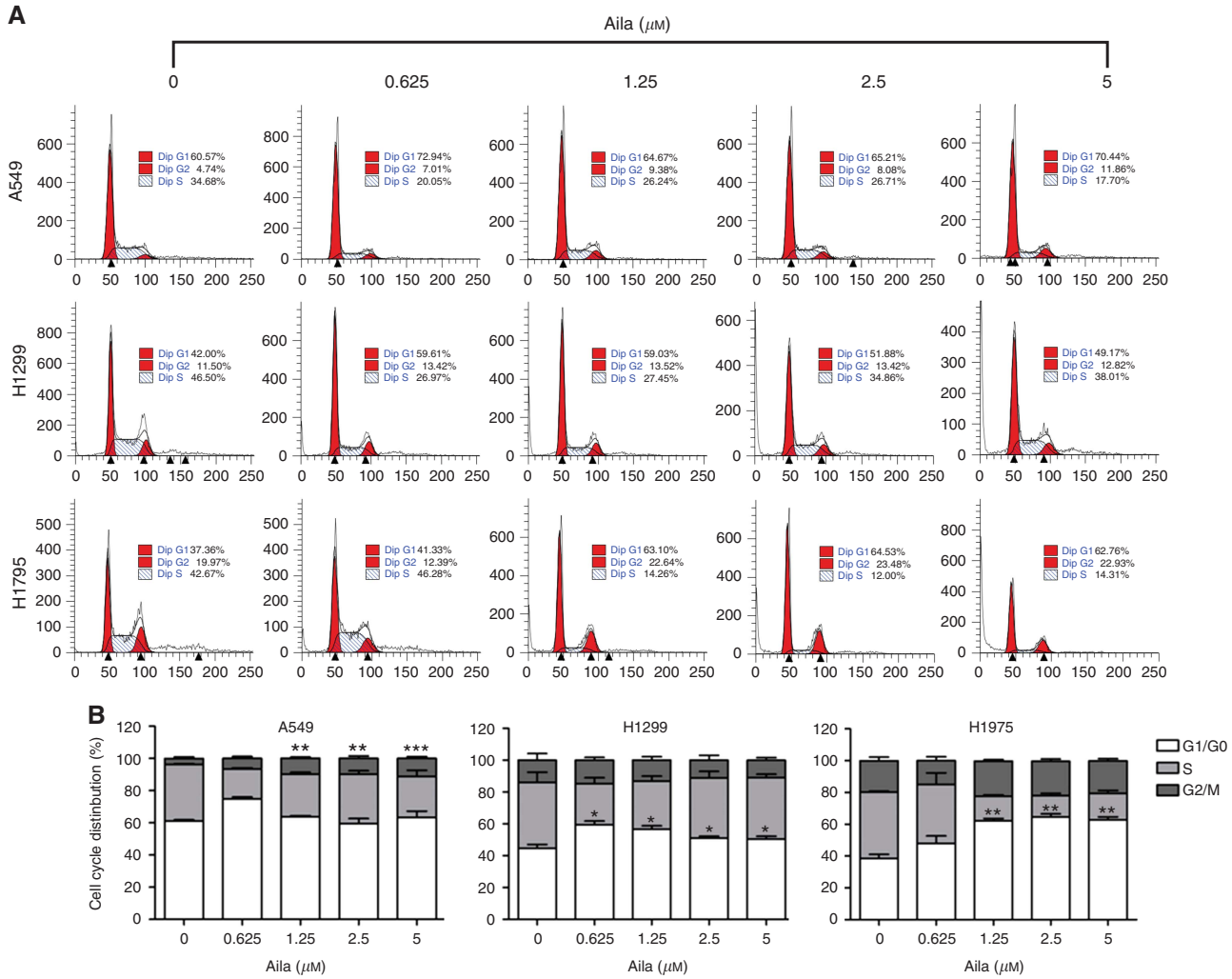

Figure 3. Aila dose-independently induces cell cycle arrest in NSCLC cells. A549, H1299 and H1975 cells were, respectively, treated with Aila at different concentrations (0, 0.625, 1.25, 2.5 and 5.0 μM) for 24 h. Cell cycle was analysed by PI staining. (**A**) Cell cycle histogram. (**B**) Data were pooled from three independent experiments. *$P<0.05$; **$P<0.01$; ***$P<0.001$.

Aila downregulates the RPA1 expression in NSCLC cells. Our data confirmed that Aila inhibited the DNA replication. We next determined whether Aila downregulated expressions of PCNA, RPA1, POLE2 and LIG1. Results showed that the expressions of PCNA and RPA1, but not POLE2 and LIG1, at the mRNA level were significantly downregulated in three types of cells (Figure 6A). This finding indicated that downregulation of PCNA and RPA1 at the mRNA level might be critical for Aila-triggered suppression of NSCLC cell growth. Therefore, we further examined expressions of PCNA and RPA1 at the protein level. Results showed that the RPA1 expression was clearly downregulated in a dose-dependent manner, while PCNA was downregulated only with high dose of Aila ($\geqslant$2.5 μM) (Figure 6B and C). Moreover, RPA1 overexpression clearly reduced the inhibitory effect of Aila on NSCLC cells (Supplementary Figure S5). These findings indicated that RPA1 was the major functional target regulated by Aila.

DISCUSSION

In the present study, Aila was found to significantly inhibit NSCLC cell growth both *in vitro* and *in vivo*, leading to prolonged survival of tumour-bearing mice. Aila dose-independently induced cell cycle arrest and induced apoptosis only in H1975 cells. In addition, Aila induced 1222 DEGs involved in 21 signal pathways, such as DNA replication. Furthermore, Aila dose-dependently inhibited DNA replication and downregulated the RPA1 expression at the mRNA and protein levels. RPA1 overexpression could reduce the inhibitory effect of Aila. These results provided solid evidence that Aila inhibited NSCLC cell growth through repressing DNA replication via downregulating RPA1.

In the current study, Aila was found to dose-independently induce classic G1 or G2/M arrest. The law of mass action shows that all pharmacological effects are concentration related and should increase in intensity with increasing dose (Aronson and Ferner, 2016). Therefore, classic G1 or G2/M phase arrest was not the major MOA of Aila due to the observed dose-independence. Aila was also found to induce apoptosis in H1975 cells, but not in H1299 and A5495 cells. Clearly, apoptosis could not well explain the inhibition in H1299 and A5495 cells. Therefore, this observation indicated that apoptosis was also not the major MOA of Aila. These findings were inconsistent with previous report that Aila inhibits liver cancer cell growth via G0/G1-phase arrest and apoptosis both *in vitro* and *in vivo* (Zhuo *et al*, 2015). This discrepancy might be caused by differences between tissues or the research limit that only one Huh7 cell line was used in that study.

BrdU incorporation is usually used to reflect the new DNA synthesis during the cell cycle S phase and the situation of DNA replication (Gratzner, 1982; Darzynkiewicz *et al*, 2011; da Silva

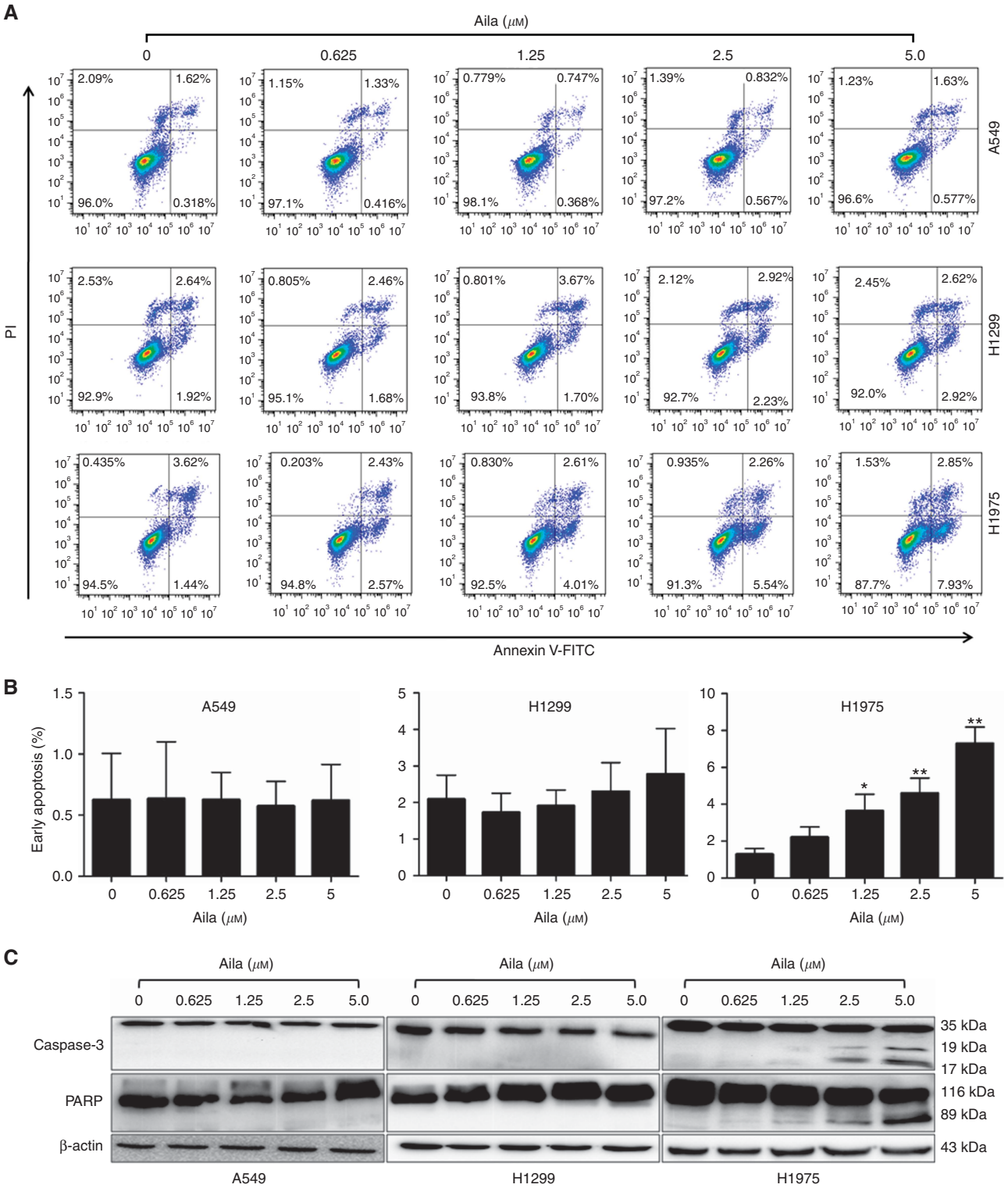

Figure 4. Aila does not induce apoptosis in all NSCLC cells. A549, H1299 and H1975 cells were, respectively, treated with Aila at different concentrations (0, 0.625, 1.25, 2.5 and 5.0 μM). (**A**) At 12 h, apoptosis was analysed by FITC-Annexin V and PI staining. (**B**) Data were pooled from (**A**). (**C**) At 24 h, Capase-3 and PARP cleavages were detected by western blotting analysis. Figure represents three independent experiments. *$P<0.05$; **$P<0.01$.

et al, 2017). In this study, BrdU flow cytometry showed that the cell cycle S phase in NSCLC cells was dramatically decreased by Aila in a dose-dependent manner. This finding confirmed our microarray result that Aila repressed DNA replication. Activation of oncogenes or loss of tumour suppressors induces sustained proliferative signalling in cancer cells, leading to replication stress and a loss of control over cell cycle (Kumar *et al*, 2017; Lin *et al*, 2017). Therefore, targeting replication stress has emerged as a new strategy in cancer therapy. Since Aila dramatically inhibited DNA replication in a dose-dependent manner, we deduced that DNA replication repression was the crucial MOA of Aila, suggesting its potential as a new anticancer reagent.

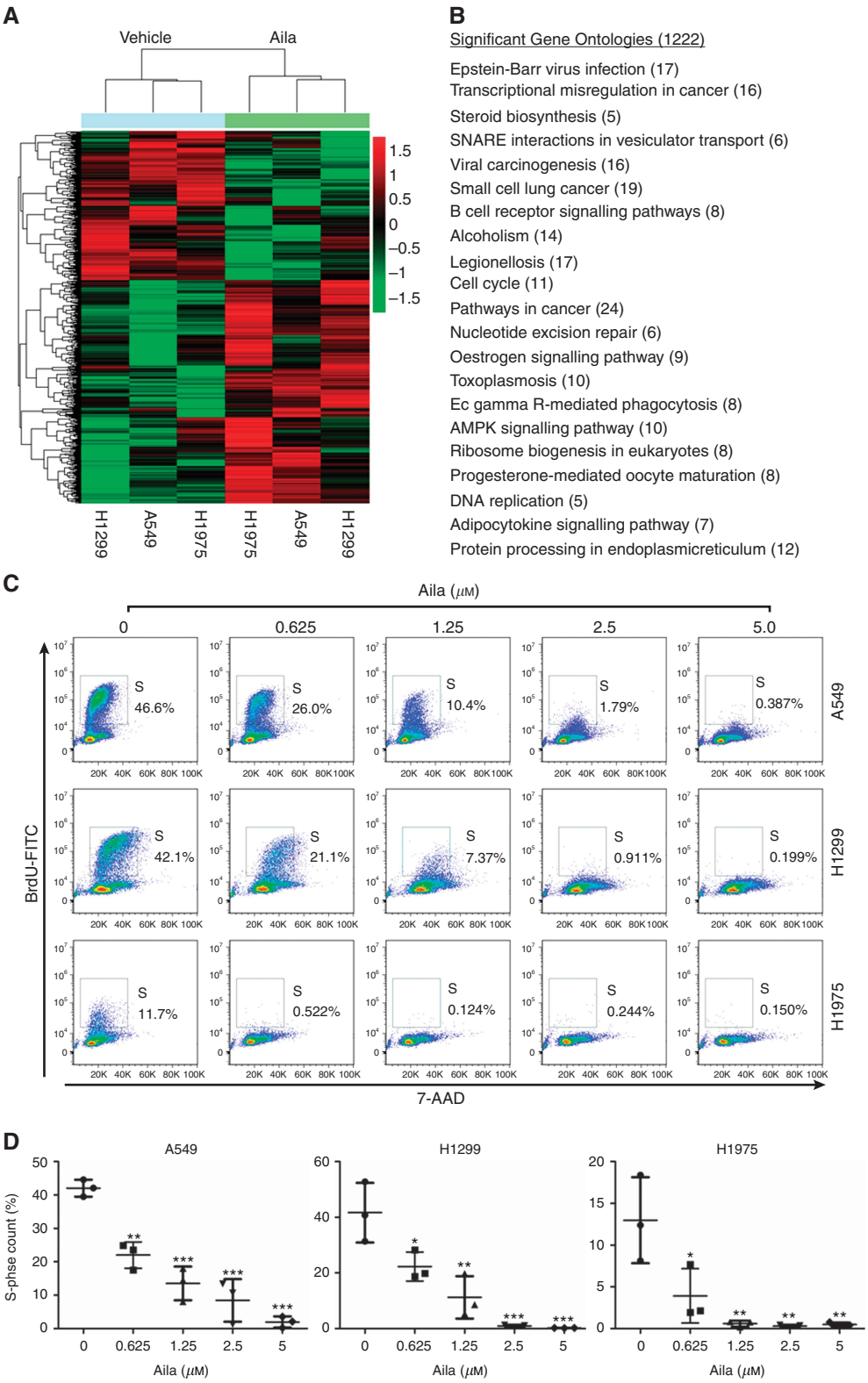

Figure 5. Aila inhibits DNA replication in NSCLC cells. (**A**) A549, H1299 and H1975 cells were respectively treated with 1.25 μM of Aila for 24 h, then a cDNA microarray was performed, and 1222 DEGs were clustered. (**B**) Signalling pathways of 1222 DEGs by GO analysis. (**C**) A549, H1299 and H1975 cells were respectively treated with Aila at different concentrations (0, 0.625, 1.25, 2.5 and 5.0 μM) for 24 h, and the percentage of S phase was determined by BrdU flow cytometry. (**D**) Data were pooled from three independent experiments. *$P<0.05$; **$P<0.01$; ***$P<0.001$.

RPA is a highly conserved heterotrimeric single-stranded DNA-binding protein complex composed of three subunits known as RPA1, RPA2 and RPA3, and it plays an essential role in DNA replication and repair (Audry *et al*, 2015). As the largest subunit of the RPA complex, RPA1 is a part of the replication fork protection complex and essential for DNA replication (Murphy *et al*, 2014; Liu and Huang, 2016). RPA1 has been shown to be a new cancer target, evidenced by that RPA1 silencing can enhance radiosensitivity and G2/M arrest in radioresistant oesophageal cancer cells (Di *et al*, 2014), and RPA1 downregulation can inhibit DNA

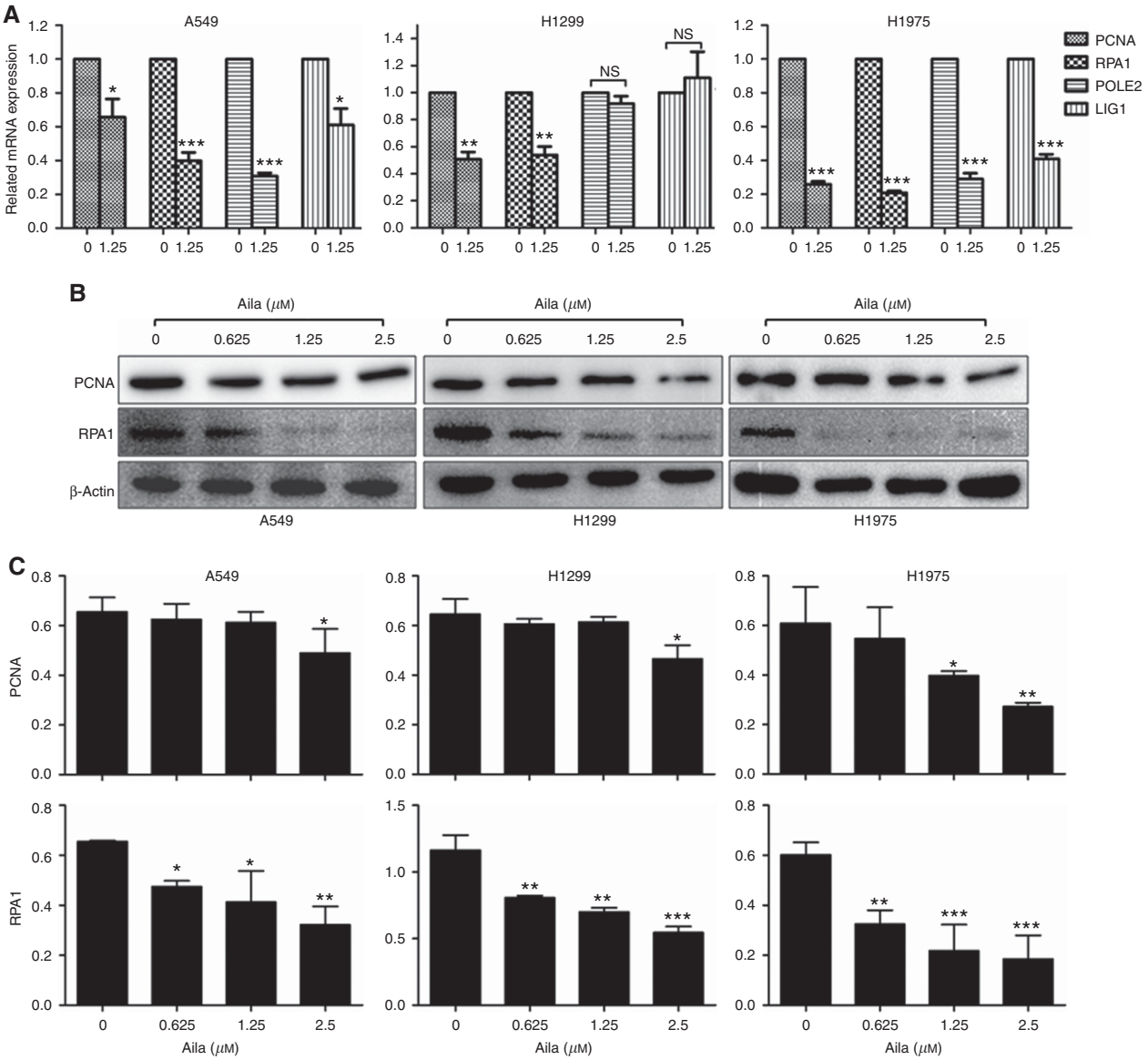

Figure 6. Aila-induced differential gene expressions were analysed by real-time PCR and western blotting analyses. (**A**) A549, H1299 and H1975 cells were respectively treated with 1.25 μM of Aila for 24 h, and then real-time PCR was performed. (**B**) A549, H1299 and H1975 cells were respectively treated with Aila at different concentrations (0, 0.625, 1.25 and 2.5 μM) for 24 h. Expressions of PCNA and RPA1 at the protein level were detected by western blotting. Figure represents three independent experiments. (**C**) Data were pooled from three independent experiments. $^{*}P<0.05$; $^{**}P<0.01$; $^{***}P<0.001$.

replication and decrease cancer cell proliferation (Zou *et al*, 2016). In this study, although the microarray result suggested that PCNA, RPA1, POLE2 and LIG1, which play critic role in DNA replication (Fanning *et al*, 2006; Yuan *et al*, 2009; Strzalka and Ziemienowicz, 2010; Howes and Tomkinson, 2012; Frugoni *et al*, 2015), were downregulated by Aila, only RPA1 was dramatically down-regulated at the mRNA and protein levels by Aila in a dose-dependent manner. RPA1 downregulation could well explain the repression of DNA replication by Aila, indicating that RPA1 was the major functional target regulated by Aila in NSCLC cells. However, detailed regulatory mechanism remains unknown and needs to be further explored. Aila has been recently shown to inhibit tumour growth of castration-resistant prostate cancer cells through targeting p23 (He *et al*, 2016b). However, it remains largely unexplored whether there is a relationship between RPA1 downregulation and p23 targeting.

Taken together, we, for the first time, showed that Aila could significantly downregulate the RPA1 expression at the mRNA and protein levels in a dose-dependent manner, resulting in the repression of DNA replication and the subsequent inhibition of NSCLC cell growth. These findings demonstratively showed that Aila had an efficient inhibitory effect on NSCLC cell growth through targeting replication stress via downregulating RPA1 expression, suggesting that Aila could be used as a promising therapeutic candidate for NSCLC patients.

ACKNOWLEDGEMENTS

This study was supported by National Natural Science Foundation of China (81473237), the Shanghai Foundation for Development of Science and Technology (14431902600), the budget project of Shanghai Municipal Education Commission (2016YSN01) and the foundation for Shanghai municipal commission of health and family planning (20154Y0167).

CONFLICT OF INTEREST

The authors declare no conflict of interest.

AUTHOR CONTRIBUTIONS

ZN performed the experiments. CY, CG, XZ, ZX, LW, SL and CZ participated in the experiments. SZ conceived the study, participated in its design and wrote the manuscript. All authors read and approved the final manuscript.

REFERENCES

Aronson JK, Ferner RE (2016) The law of mass action and the pharmacological concentration-effect curve: resolving the paradox of apparently non-dose-related adverse drug reactions. *Br J Clin Pharmacol* **81**: 56–61.

Audry J, Maestroni L, Delagoutte E, Gauthier T, Nakamura TM, Gachet Y, Saintome C, Geli V, Coulon S (2015) RPA prevents G-rich structure formation at lagging-strand telomeres to allow maintenance of chromosome ends. *EMBO J* **34**: 1942–1958.

Chen W, Zheng R, Baade PD, Zhang S, Zeng H, Bray F, Jemal A, Yu XQ, He J (2015) Cancer statistics in China, 2015. *CA Cancer J Clin* **66**: 115–132.

Cragg GM, Newman DJ (2013) Natural products: a continuing source of novel drug leads. *Biochim Biophys Acta* **1830**: 3670–3695.

da Silva MS, Munoz PA, Armelin HA, Elias MC (2017) Differences in the detection of BrdU/EdU incorporation assays alter the calculation for G1, S, and G2 phases of the cell cycle in trypanosomatids. *J Eukaryot Microbiol;* e-pub ahead of print 4 March 2017; doi:10.1111/jeu.12408.

Darzynkiewicz Z, Traganos F, Zhao H, Halicka HD, Li J (2011) Cytometry of DNA replication and RNA synthesis: historical perspective and recent advances based on 'click chemistry'. *Cytometry A* **79**: 328–337.

Di Z, Sanyuan S, Hong L, Dahai Y (2014) Enhanced radiosensitivity and G2/M arrest were observed in radioresistant oesophageal cancer cells by knocking down RPA expression. *Cell Biochem Biophys* **70**: 887–891.

Fanning E, Klimovich V, Nager AR (2006) A dynamic model for replication protein A (RPA) function in DNA processing pathways. *Nucleic Acids Res* **34**: 4126–4137.

Frugoni F, Dobbs K, Felgentreff K, Aldhekri H, Al Saud BK, Arnaout R, Ali AA, Abhyankar A, Alroqi F, Giliani S, Ojeda MM, Tsitsikov E, Pai SY, Casanova JL, Notarangelo LD, Manis JP (2015) A novel mutation in the POLE2 gene causing combined immunodeficiency. *J Allergy Clin Immunol* **137**: 635–638 e1.

Gratzner HG (1982) Monoclonal antibody to 5-bromo- and 5-iododeoxyuridine: a new reagent for detection of DNA replication. *Science* **218**: 474–475.

He XR, Han SY, Li PP (2016a) Recent highlights of Chinese medicine for advanced lung cancer. *Chin J Integr Med* **23**: 323–330.

He Y, Peng S, Wang J, Chen H, Cong X, Chen A, Hu M, Qin M, Wu H, Gao S, Wang L, Wang X, Yi Z, Liu M (2016b) Ailanthone targets p23 to overcome MDV3100 resistance in castration-resistant prostate cancer. *Nat Commun* **7**: 13122.

Howes TR, Tomkinson AE (2012) DNA ligase I, the replicative DNA ligase. *Subcell Biochem* **62**: 327–341.

Kim HM, Kim SJ, Kim HY, Ryu B, Kwak H, Hur J, Choi JH, Jang DS (2015) Constituents of the stem barks of Ailanthus altissima and their potential to inhibit LPS-induced nitric oxide production. *Bioorg Med Chem Lett* **25**: 1017–1020.

Kumar S, Peng X, Daley J, Yang L, Shen J, Nguyen N, Bae G, Niu H, Peng Y, Hsieh HJ, Wang L, Rao C, Stephan CC, Sung P, Ira G, Peng G (2017) Inhibition of DNA2 nuclease as a therapeutic strategy targeting replication stress in cancer cells. *Oncogenesis* **6**: e319.

Lin AB, McNeely SC, Beckmann RP (2017) Achieving precision death with cell cycle inhibitors that target DNA replication and repair. *Clin Cancer Res* **23**: 3232–3240.

Liu T, Huang J (2016) Replication protein A and more: single-stranded DNA-binding proteins in eukaryotic cells. *Acta Biochim Biophys Sin (Shanghai)* **48**: 665–670.

Murphy AK, Fitzgerald M, Ro T, Kim JH, Rabinowitsch AI, Chowdhury D, Schildkraut CL, Borowiec JA (2014) Phosphorylated RPA recruits PALB2 to stalled DNA replication forks to facilitate fork recovery. *J Cell Biol* **206**: 493–507.

Strzalka W, Ziemienowicz A (2010) Proliferating cell nuclear antigen (PCNA): a key factor in DNA replication and cell cycle regulation. *Ann Bot* **107**: 1127–1140.

Tada Y, Grossart HP (2013) Community shifts of actively growing lake bacteria after N-acetyl-glucosamine addition: improving the BrdU-FACS method. *ISME J* **8**: 441–454.

Wang R, Xu Q, Liu L, Liang X, Cheng L, Zhang M, Shi Q (2016) Antitumour activity of 2-dihydroailanthone from the bark of Ailanthus altissima against U251. *Pharm Biol* **54**: 1641–1648.

Yuan J, Ghosal G, Chen J (2009) The annealing helicase HARP protects stalled replication forks. *Genes Dev* **23**: 2394–2399.

Zheng H, He S, Liu R, Xu X, Xu T, Chen S, Guo Q, Gao Y, Hua B (2017) Chinese patent medicine Fei-Liu-Ping ointment as an adjunctive treatment for non-small cell lung cancer: protocol for a systematic review. *BMJ Open* **7**: e015045.

Zhuo Z, Hu J, Yang X, Chen M, Lei X, Deng L, Yao N, Peng Q, Chen Z, Ye W, Zhang D (2015) Ailanthone inhibits Huh7 cancer cell growth via cell cycle arrest and apoptosis in vitro and in vivo. *Sci Rep* **5**: 16185.

Zou Z, Ni M, Zhang J, Chen Y, Ma H, Qian S, Tang L, Tang J, Yao H, Zhao C, Lu X, Sun H, Qian J, Mao X, Liu Q, Zen J, Wu H, Bao Z, Lin S, Sheng H, Li Y, Liang Y, Chen Z, Zong D (2016) miR-30a can inhibit DNA replication by targeting RPA1 thus slowing cancer cell proliferation. *Biochem J* **473**: 2131–2139.

Supplementary Information accompanies this paper on British Journal of Cancer website (http://www.nature.com/bjc)